Spectral Signatures of Carbonate Rocks Surrounding The Nanisivik MVT Zn-Pb Mine and Implications of Hyperspectral Imaging for Exploration in Arctic Environments

P. Budkewitsch[1] , K. Staenz[1] , J. Secker[1] , A. Rencz[2] and D. Sangster[2]

[1] Applications Development Section
Canada Centre for Remote Sensing
588 Booth Street
Ottawa, Ontario, K1A 0Y7
[2]Geological Survey of Canada
601 Booth Street
Ottawa, Ontario, K1A 0E8

Abstract. *Spectral unmixing techniques of hyperspectral data have been developed together with endmember selection procedures to successfully map the distribution of minerals and alteration for mineral exploration. A particular challenge for mineral mapping in Canada is the application of these techniques to arctic environments. The objective of this study is to validate the use of spectral unmixing techniques for creating mineral abundance maps of the exposed rock in the Borden Rift Basin of northern Baffin Island using hyperspectral imaging data. Results indicate potential to distinguish limestone from dolostone using spectral reflectance properties in the 2050-2450 nm region of the Short-wave Infra-red (SWIR). Limestones (calcite-dominated) typically show strongest absorption near 2330 nm whereas dolostones (dolomite-dominated) exhibit greatest absorption near 2310 nm. This* ca*. 20 nm difference raises the possibility that these two rock types can be distinguished in hyperspectral imaging data.*

A quantitative analysis is presented, describing the geological significance of endmembers extracted from Probe-1 hyperspectral data as revealed in fraction maps from unmixing results. Validation of the unmixing results with ground reference information illustrates the potential of using hyperspectral units as an indicator for mapping the occurrence of limestone and dolostone and the mapping of dolomitized alteration zones.

Introduction

Over the last few decades, optical remote sensing has traditionally consisted of single channel panchromatic or multispectral imaging systems which are able to collect data from broad spectral bands. More recently the technology has advanced to include hyperspectral imaging systems that are able to acquire radiance data in narrow, contiguous spectral bands and record well over a hundred bands from each instantaneous field-of-view (FOV). With this plethora of data to analyse, spectral matching and unmixing techniques have been developed together with procedures for identifying and mapping minerals for geoscience applications. Such studies have been quite successful in

arid and semi-arid regions at low latitudes with sparse vegetation cover (*e.g*., Mustard and Pieters, 1986; Gillespie *et al*., 1990; Boardman and Huntington, 1996; Neville *et al*., 1998; Staenz *et al*., 1999) and the results have attracted the interest of geologists in hyperspectral work for resource exploration. Mineral mapping is often referred to in place of lithological mapping because many minerals have distinct spectral response characteristics and spectral identification of endmembers is usually accomplished through methods of matching observed spectral signatures with those of known minerals.

This paper presents some preliminary results of a hyperspectral imaging project being undertaken by the Canada Centre for Remote Sensing in the Canadian Arctic. The objective is to demonstrate the potential of hyperspectral imaging for mapping and mineral exploration at higher latitudes where solar elevation angles are significantly lower and where direct exposure of bedrock may be occluded by a high proportion of biogenic cover. A site representing a High Arctic ecozone was selected in the Borden Rift Basin, on northern Baffin Island. Unlike the sparsely vegetated deserts of lower latitudes, tundra vegetation may cover a large proportion of the terrain. This vegetation, including lichens and mosses, can complicate the extraction of spectra related to bedrock which is required for the production of mineral maps. Outcrop in tundra environments are typically encrusted with lichens of various kinds. It is often noted, however, that carbonate rocks are significantly less colonised than other rock types.

We report on the potential of hyperspectral imaging to support geological mapping and exploration efforts in these remote regions, and present an example where spectral unmixing of hyperspectral data is able to distinguish limestone from dolostone. The discrimination of these two carbonate rocks is possible due to the different spectral reflectance properties of calcite and dolomite in the SWIR region of the spectrum. Limestones (calcite-dominated) typically show the strongest absorption at a wavelength near 2330 nm whereas dolostones (dolomite-dominated) exhibit greatest absorption near 2310 nm (*cf*., Grove *et al*., 1992). This 20 nm difference raises the possibility that these two rock types can be distinguished in hyperspectral imaging data, provided that sufficient spectral sampling, appropriate bandwidth and an acceptable signal-to-noise characterises the sensor employed.

Site Description

The Borden Rift Basin of northern Baffin Island (N73°/W84.5°) is located in a High Arctic ecozone where vegetation is sparse and snow-free conditions exist for less than two or three months a year. The geology consists of Late Proterozoic sedimentary rocks deposited within a deepening rift basin. Jackson and Sangster (1987) describe two locally mapped formations. The Society Cliffs Formation forms a thick sequence of laminated dolostones and the Victor Bay Formation conformably overlies the former with deep basinal shales shallowing upward with interbedded limestones and subtidal dolostones in the upper part. An angular unconformity separates these older Proterozoic units from a younger cover of Paleozoic cross-bedded quartz sandstones and redbeds that belong to the Admirality Group (Jackson and Sangster, 1987). The dolostones of the Society Cliffs Formation host an economic concentration Zn-Pb mineralisation mined at Nanisivik.

Only a few other sub-economic Zn-Pb occurrences are known from other parts of the basin.

Block faulting during various periods has resulted in minor warping and low angle dips of the strata. The magnitude of stratigraphic offsets varies from a few metres to several hundred metres. The terrain can be generally characterised as an elevated plateau, divided into northwest-trending ranges and basins. Bedrock or felsenmeer exposures are common in the high ground and are generally carbonates or quartzites. Reworked glacial deposits and mossy grasslands occupy the broad valleys which are commonly underlain by less resistant shale-dominated units. Both limestone and dolostone bedrock units are generally free of vegetation and lichen cover whereas the well-cemented quartzites and gabbro dykes frequently exhibit a high proportion of encrusting lichen cover. Each of these lithological can be identified in the hyperspectral data and distinguished with reasonable fidelity, according to the geological maps and follow-up verification in the field.

Data Acquisition and Processing

Ground-based reflectance spectra

Field measurements using a GER3700™ portable field spectrometer manufactured by Geophysical Environmental Research Corporation (Millbrook, New York) were collected from the study site for the variety of rock types encountered in the area. The instrument was configured with a 3- or 10-degree FOV lens and data is recorded over narrow spectral bands from 400 to 2500 nm. Measurements were made at different heights above the ground targets to yield various ground FOV diameters in the range of 2 to 40 cm. All measurements were made while the sky was free of all clouds in the vicinity of the sun and a Spectralon™ reference panel was used to normalise radiance measurements to ground reflectance. The resulting reflectance spectra were corrected for the wavelength and angular dependency of the reference panel's reflectance (Secker *et al*., in press). Multiple measurements of a given sample were averaged to yield a mean spectrum for that sample. These measurements of relatively pure rock material are used to compare with the extracted endmember spectra from the airborne hyperspectral data. Samples were also collected for thin-section and geochemical analysis. The results of this part of the project will be reported elsewhere.

Airborne hyperspectral data

Six flight lines of hyperspectral data over selected areas of the Borden Rift basin were obtained with the Probe-1 sensor on the dates of July 27 and 29, 1999. This paper describes some results from a sample data set extracted from one of the flight lines near the Nanisivik Mine. The mission and atmospheric correction parameters used for the analysis are summarised in Table 1. Probe-1 is an airborne visible and near infra-red (VNIR) and SWIR hyperspectral imaging system with 128 spectral bands spanning the wavelength range from 440 nm to 2450 nm. Bandwidths are between 11 nm in the VNIR range and up to 22 nm in the SWIR region (Secker *et al*., in press). The across track image consists of 512 pixels collected over a 60-degree FOV, which for the altitude of

this mission corresponds to a ground width of about 3.3 km and 6.5-m pixels. Whenever possible, flight lines were orientated as close as possible to the solar azimuth angle to minimise bi-directional reflectance effects. The sensor is mounted on a three-axis gyro-stabilised platform that compensates for the effects of aircraft motion (for up to 5 degrees on each axis) and thus corrections for pitch, roll and yaw were not required to this data set.

For the calibration of Probe-1 hyperspectral data, first the dark current was subtracted and then pre-flight laboratory calibration coefficients supplied by the operators were used to convert the raw data from digital numbers (DN) to radiance values, with units of $\mu W\ cm^{-2}\ nm^{-1}\ sr^{-1}$.

The raw at-sensor radiance spectra were converted to surface reflectance via an atmospheric correction using the MODTRAN3 radiative-transfer code (Berk *et al*., 1989; Anderson *et al*., 1995) implemented using a LUT approach in ISDAS (Staenz and Williams, 1997). Inputs to the MODTRAN3 routine require mission-specific and sensor-specific parameters, and model-specific choices for atmospheric properties. These are summarised in Table 1. Using MODTRAN3, the atmospheric transmission was calculated over the full wavelength range of the sensor, and then resampled to match the characteristics of the Probe-1 sensor.

Table 1. Airborne mission and MODTRAN3 model parameters for atmospheric correction of the Probe-1 hyperspectral data.

Probe-1 Mission Parameters	
Date	**1999-07-27**
GMT	**18:50:00**
Aircraft heading	**17°**
Sensor tilt angle	**0°**
Sensor altitude (above sea level)	**3.300 km**
Pixel size	**6.5 m**
MODTRAN3 Model Parameters	
Atmospheric model	**Subarctic Summer**
Aerosol model	**Continental (rural)**
Solar zenith angle	**54.69°**
Solar azimuth angle	**198.96°**
Mean terrain elevation	**+360 m**
Water vapour	**0.85 g/cm^2**
Ozone column	**0.346 cm-atm**
CO_2 mixing ratio	**357.5 ppm**
Visibility	**50 km**

The amount of atmospheric water vapour from the Subarctic Summer model of 2.102 g/cm^2 was replaced with an average value of 0.85 g/cm^2 estimated from airborne hyperspectral data by sampling several individual pixels, using a method which models

the combined strength of the 940 nm and 1130 nm water vapour absorption lines in the spectra (Gao and Goetz, 1990; Green *et al*., 1991; Staenz and Williams, 1997).

Endmember Selection and Spectral Unmixing

In order to create image maps to illustrate the proportion and spatial distribution of different rock types, a constrained linear spectral unmixing technique (Adams *et al*., 1986; Shimabukuru and Smith, 1991; Boardman, 1995) was applied. The basic principal of spectral unmixing is to use a linear combination of a set of "endmember" spectra to unmix the composite spectrum into endmember fractions (between 0 and 1) for each pixel in the data set. Ideally, endmembers are relatively pure material that can be found in the scene being analysed. For example, in the Nanisivik area, water, vegetation, bedrock and unconsolidated deposits comprise the terrain and would describe four good endmembers. In practice, the multidimensional nature of hyperspectral data allows for a far greater discernment of endmember types.

One of the criteria for endmember determination is that each of these materials possess a characteristic spectra. The endmembers needed for the unmixing of the entire data can be selected in various ways. For the results of unmixing analysis described here, endmembers were selected directly from the airborne hyperspectral set using an automatic approach called Iterative Error Analysis (IEA) developed at CCRS. The method relies on being able to find a pixel or group of pixels which correspond to that area on the ground composed entirely or almost entirely of the pure endmember material. The reader is referred to Szeredi *et al.* (submitted) for more details on the IEA methodology.

In this analysis, a Probe-1 data "cube" of approximately 512x512 pixels was extracted from one of the flight lines and only 23 bands, in the 2050 to 2450 nm wavelength range, of data was utilised for the endmember selection and spectral unmixing procedure. Figure 1a is a near true colour image derived from the visible bands of the Probe-1 dataset. A simplified geological map corresponding to the area is shown in Figure 1b showing the distribution of four mapped units. The Society Cliffs and Upper Victor Bay Formations are dolostones, limestone is locally exposed within the Lower Victor Bay and the Admirality Group consists of poorly indurated terrigenous quartz sandstones and red beds. Abundant outcrop and high terrain elevation is at the north and south ends of the site whereas the central part is a broad valley characterised by a pavement of pebbles and cobbles of mixed lithology, thin felsenmeer and relatively few outcrops (Figure 1a).

For the unmixing procedure in the Nanisivik site described here, 25 endmembers was arbitrarily chosen (to be certain not to omit any significant materials) as the number of endmembers to extract and unmix for. Each of these "pure" endmember spectra are determined from a maximum of 25 pixels in the data set. Once all the endmembers were found, the hyperspectral data for the area was unmixed using those endmembers. We examined the characteristic spectra and fraction maps from the unmixing results generated from each endmember. Spectral absorption features in the Probe-1 endmember spectra were visually compared to the corresponding ground-based reflectance spectra

measurements made with the GER3700™ spectrometer to determine the type of endmember material found in the unmixing results

Of the 25 endmembers extracted using the IEA method, approximately half are of geological interest. In addition to water, snow, dark shade and common tundra vegetation endmembers, some of the endmembers found corresponded to pixels where roads or the roof tops of mine buildings were located. Because of bi-directional effects caused by local variations in the topography, the IEA procedure extracted spectrally similar endmembers that were only differentiated by their amplitudes. At this time, a digital elevation model was not used to help correct for these effects, however these spectrally similar endmembers were grouped together and their corresponding fraction maps added.

Results and Discussion

The summed fraction maps are shown as Figures 1c,d,e. Figure 1c contains three endmembers with similar flat spectral profiles corresponding to the spectral response of the mineral quartz in this wavelength range. The fraction map corresponds very well to outcrops of the Admirality Group. The fraction map of Figure 1d is the summation of six endmembers, each of which exhibits a similar spatial co-occurrence and characteristic carbonate absorption features. A high correlation to the mapped occurrence of the Victor Bay Formation (Upper and Lower) is observed. Five of these individual endmembers are illustrated separately in Figures 2b-f and discussed in more detail below. The last endmember fraction map (Figure 1e) shows an overall weak abundance and some spatial distribution to the Society Cliffs Formation as well as along the broad valley. The spectral reflectance of this material is less than 5% and affected by noise at this low amplitude. Although the petroliferous dolostones of the Society Cliffs are a much darker gray than the carbonate rocks of the Victor Bay Formation, unfavourable illumination conditions on the west sloping topography in this area may also be a cause for the difficulty in extracting an appropriate endmember for this unit.

Discrimination of limestone and dolostone in hyperspectral data

To facilitate comparisons, the fraction map of Figure 1d is reproduced as Figure 2a, beside the constituent endmember fraction maps (Figures 2b-f). The fraction map of endmember #19 is not shown, but has a similar distribution to endmember #13 (Figure 2f). Endmembers #1 and 11 (Figure 2b,c) have similar Probe-1 spectral reflectance signatures, as shown in Figure 3a, and are recognised as dolostone according to the absorption feature minima near 2310-2320 nm and asymmetrical shape characteristic of the mineral dolomite. It is interesting to note the strong spatial correlation to the Upper Victor Bay Formation in Figure 1b.

Endmembers # 6, 8 and 13 (Figures 2d-f) have a similar spatial distribution and map well to the location of the Lower Victor Bay Formation (Figure 1b). In Figure 3b each of the three endmembers have grossly similar Probe-1 spectral reflectances, offset only by 1-2% in amplitude. Their shape and absorption feature minima near 2330-2340 nm is indicative of the mineral calcite and, therefore, the rocks have a strong likelihood of being limestones. Many of these predicted locations for limestone and dolostone were verified

in the field using a dilute solution of HCl to test for positive (calcite) or negative (dolomite) effervescence. Further geochemical analysis are underway to quantify these findings.

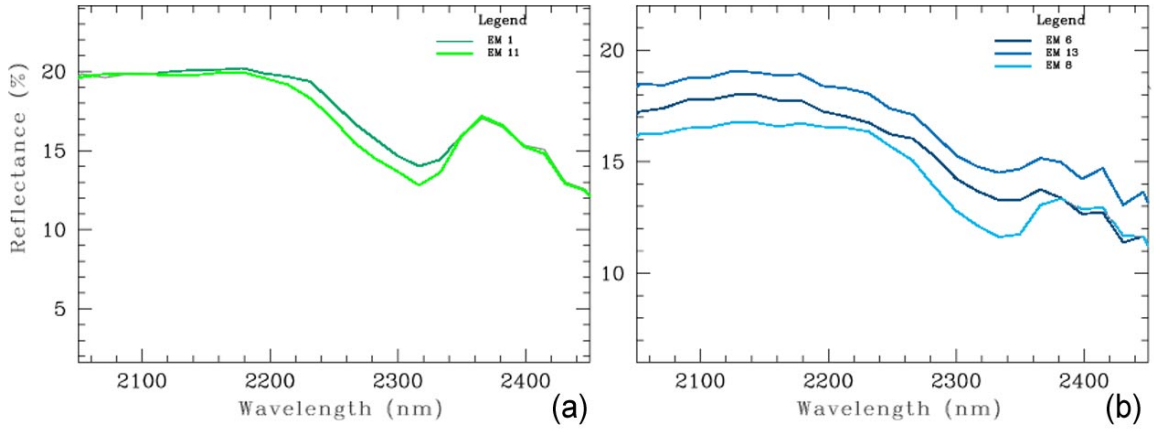

Figure 3. Graphs of Probe-1 SWIR spectral characteristics of **(a)** the two dolostone endmembers and **(b)** the three limestone endmembers illustrated in Figures 2b-f.

Conclusions and Further Work

Results from our preliminary investigation of Probe-1 hyperspectral data in the Nanisivik area indicates that analysis of extracted endmembers and spectral unmixing techniques can be successfully employed for the identification of different rock units in arctic environments. Limestone and dolostone can be successfully distinguished and results presented indicate promise for discriminating amongst different kinds of dolostone and limestone. At this time, we wish to emphasise that unmixing analysis of hyperspectral imaging data produce fraction maps of "hyperspectral units" whose results are not entirely correlative to lithological or stratigraphic units as mapped by geologists. The findings indicate that this methodology may allow for the identification of areas of dolomitisation, which is important for mapping alteration zones in carbonate rocks and of interest for mineral exploration in MVT settings.

Bi-directional reflectance has a profound effect on the types of endmember spectral signatures extracted from the data. This is due to the low solar elevation angles (typically less than 40°) at these high latitudes, augmented by the variable slope-and-aspect of the terrain and finally the 60° FOV of the Probe-1 (and other airborne) hyperspectral imaging system. Through examination of ground spectral measurements, some of the amplitude and magnitude differences can be attributed to mineral grain size. Other reasons for differences in similar spectral signature classes are likely to be discovered as further work to understand these differences continues.

Acknowledgements

The authors wish to thank John Gingerich (Noranda Mining and Exploration Inc.) for facilitating logistics for the Probe-1 data collection campaign over Baffin Island. Logistical support from the Polar Continental Shelf Project for field validation is gratefully acknowledged. Ron Sutherland (Nanisivik Mine) is thanked for stimulating discussions and for sharing his expert knowledge on the geology of the area. CCRS acknowledges the generous financial support for this project by Barrick Gold Corp., Cameco, Cominco Ltd., De Beers Consolidated Mines Ltd., Falconbridge Limited, Noranda Mining and Exploration Inc., and Placer Dome Exploration Inc. The authors sincerely appreciate the cooperation of the Hamlet and Arqvartuuq Services Ltd. of Arctic Bay, the assistance of Larry Oyukuluk and the courtesy of the staff at the Nanisivik Mine during the summer of 1999. This is Polar Continental Shelf Project contribution #033-00.

References

Adams, J.B., Smith, M.O., and Johnson, P.E. 1986. Spectral Mixture Modelling: A New Analysis of Rock and Soil Types at the Viking Lander 1 Site. *Journal of Geophysical Research*, **91**, pp. 8098-8112.

Anderson, G.P., Wong, J., and Chetwynd, J.H. 1995. MODTRAN3: An Update on Recent Validations Against Airborne High Resolution Interferometer Measurement. Summaries of the Fifth Annual JPL Airborne Earth Science Workshop, Jet Propulsion Laboratory, Pasadena, CA, **JPL Publication 95-1**, Vol. 1, pp. 5-8.

Berk, A., Bernstein, L.S., and Robertson, D.C. 1989. MODTRAN: A Moderate Resolution Model for LOWTRAN7. **Final Report**, GL-TR-0122, AFGL, Hanscom AFB, MD, 37 p.

Boardman, J.W. 1995. Analysis, Understanding and Visualization of Hyperspectral Data as Convex Sets in n-Space. Proceedings of the International SPIE Symposium on Imaging Spectrometry, **SPIE** Vol. **2480**, Orlando, FL., pp. 23-36.

Boardman, J.W., and Huntington, J.F. 1996. Mineral Mapping with 1995 AVIRIS Data. Summaries of the Sixth Annual JPL Airborne Earth Science Workshop, Pasadena, CA, **JPL Publication 96-4**, Vol. 1, pp. 9-11.

Gao, B.-C., and Goetz, A.F.H. 1990. Column Atmospheric Water Vapour and Vegetation Liquid Water Retrievals from Airborne Imaging Spectrometer Data. *Journal of Geophysical Research*, **95**(D4), pp. 3549-3564.

Gillespie, A.R., Smith, M.O., Adams, J.B., Willies, S.C., Fischer, A.F., and Sabol, D.E. 1990. Interpretation of Residual Images: Spectral Mixture Analysis of AVIRIS Images, Owens Valley, California. Proceedings of the Second Airborne Visible/Infrared Imaging Spectrometer (AVIRIS) Workshop, Pasadena, CA, **JPL Publication 90-54**, pp. 243-270.

Green, R.O., Conel, J.E., Margolis, J.S., Brugge, C.J., and Hoover, G.L. 1991. An Inversion Algorithm for Retrieval of Atmospheric and Leaf Water Absorption from AVIRIS Radiance with Compensation for Atmospheric Scattering. Proceedings of the Third Annual JPL Airborne Earth Science Workshop, Pasadena, CA, **JPL Publication 91-28**, Vol. 1, pp. 51-61.

Grove, C.I., Hook, S.J. and Paylor II, E.D. 1992. Laboratory Reflectance Spectra of 160 Minerals, 0.4 to 2.5 Micrometers. National Aeronautics and Space Administration, Jet Propulsion Laboratory, California Institute of Technology, Pasadena, CA, **JPL Publication 92-2**, 406p.

Jackson, G.D. and Sangster, D.F. 1987. Geology and Resource Potential of a Proposed National Park, Bylot Island and Northwest Baffin Island, Northwest Territories. Geological Survey of Canada, Ottawa, ON, **Paper 87-17**, 31p.

Mustard, J.F., and Pieters, C.M. 1986. Abundance and Distribution on Mineral Components Associated with Moses Rock (Kimberlite) Diatreme. Proceedings of the Second Airborne Imaging Spectrometer Data Analysis Workshop, Pasadena, CA, **JPL Publication 86-35**, pp. 81-85.

Neville, R.A., Nadeau., C., Levesque, J., Szeredi, T., Staenz, K., Hauff, P., and Borstad, G.A. 1998. Hyperspectral Imagery for Mineral Exploration: Comparison of Data from Two Airborne Sensors. Proceedings of the International SPIE Symposium on Imaging Spectrometry, San Diego, CA, **SPIE** Vol. **3438**, pp. 74-82.

Secker, J., Staenz, K., Gauthier, R.P., and Budkewitsch, P. (in press). Vicarious Calibration of Hyperspectral Sensors in Operational Environments, *Remote Sensing of Environment*.

Shimabukuru, Y.E., and Smith, J.A. 1991. The Least Squares Mixing Models to Generate Fraction Images Derived From Remote Sensing on Multispectral Data. *IEEE Transactions on Geoscience and Remote Sensing*, **29**, pp. 16-20.

Staenz, K., and Williams, D.J. 1997. Retrieval of Surface Reflectance from Hyperspectral Data Using a Look-Up Table Approach. *Canadian Journal of Remote Sensing*, **23**(4), pp. 354-368.

Staenz, K., Neville, R.A., Levesque, J., Szeredi, T., Singhroy, V., Borstad, G.A., and Hauff, P. 1999. Evaluation of *casi* and SFSI Hyperspectral Data for Environmental and Geological Applications – Two Case Studies. *Canadian Journal of Remote Sensing*, **25**(3), pp. 311-322.

Szeredi, T., Staenz, K., and Neville, R.A. (submitted). Automatic Endmember Selection: Part I Theory. *Remote Sensing of Environment*.

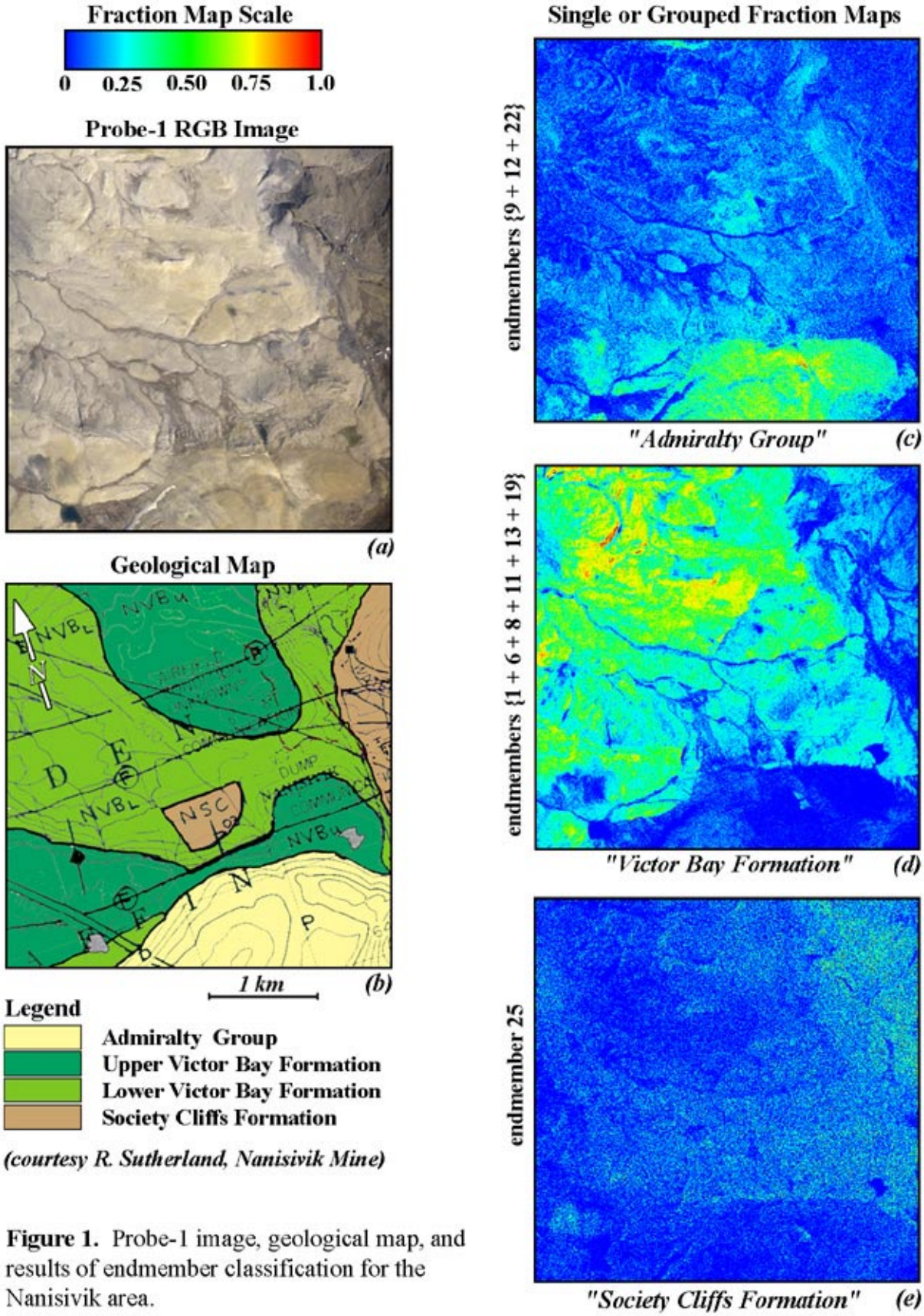

Figure 1. Probe-1 image, geological map, and results of endmember classification for the Nanisivik area.

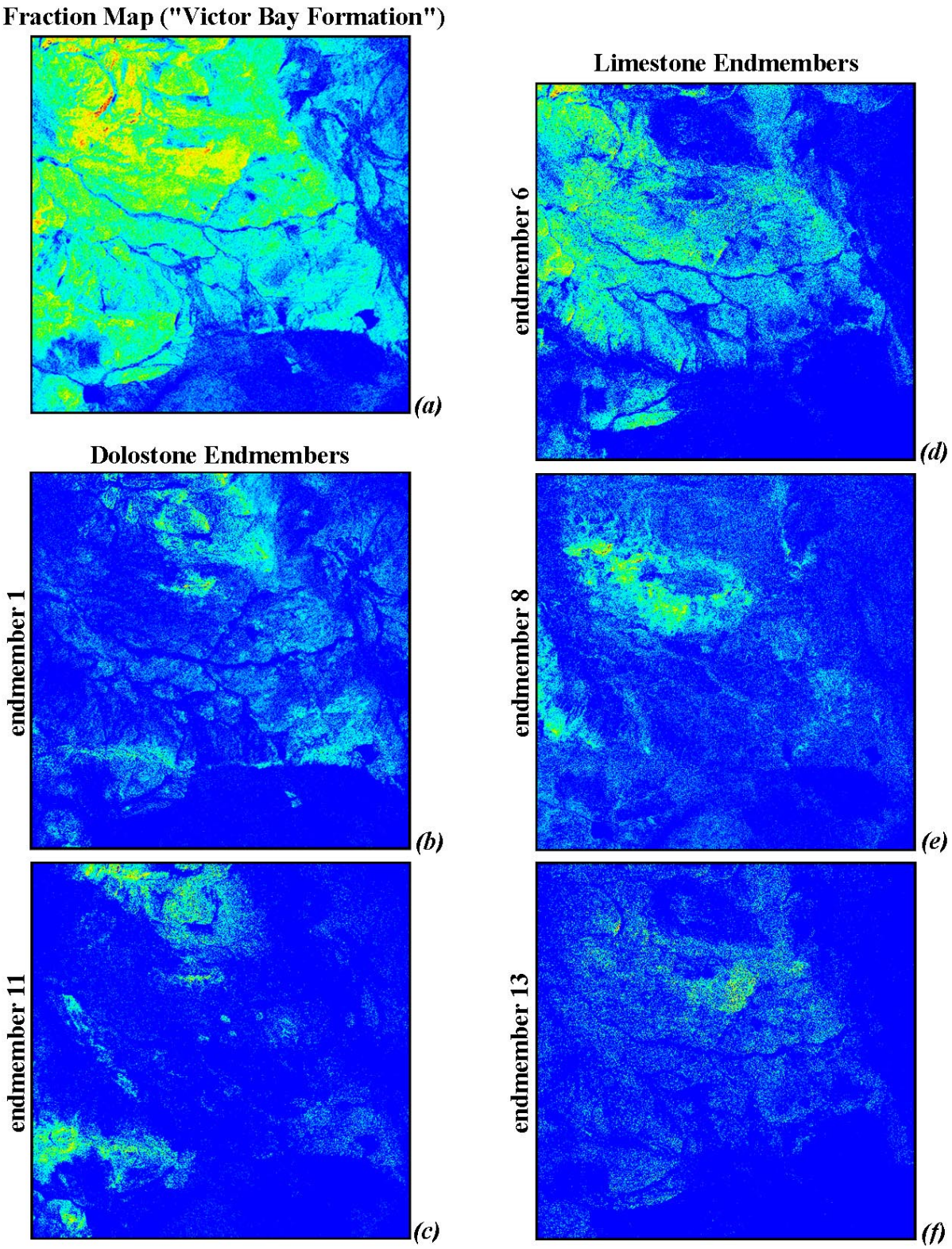

Figure 2: Fraction maps of two dolostone and three limestone endmembers corresponding to the Upper and Lower Victor Bay Formation respectively.